[33] Terry NH, Tucker SL, Travis EL. Residual radiation damage in murine lung assessed by pneumonitis. Int J Radiat Oncol Biol Phys 1988;14:929–38.
[34] Okamoto Y, Murakami M, Yoden E, et al. Reirradiation for locally recurrent lung cancer previously treated with radiation therapy. Int J Radiat Oncol Biol Phys 2002;52:390–6.
[35] Fowler JF. The first James Kirk memorial lecture. What next in fractionated radiotherapy? Br J Cancer Suppl 1984;6:285–300.
[36] Tucker SL. Tests for the fit of the linear-quadratic model to radiation isoeffect data. Int J Radiat Oncol Biol Phys 1984;10:1933–9.
[37] Steel GG. Basic clinical radiobiology, text book. Hodder Arnold, ISBN 0-340-80783-0 3rd ed. 1997.
[38] Guerrero M, Li XA. Extending the linear-quadratic model for large fraction doses pertinent to stereotactic radiotherapy. Phys Med Biol 2004;49:4825–35.
[39] Park C, Papiez L, Zhang S, et al. Universal survival curve and single fraction equivalent dose: useful tools in understanding potency of ablative radiotherapy. Int J Radiat Oncol Biol Phys 2008;70:847–52.

ELSEVIER

Int. J. Radiation Oncology Biol. Phys., Vol. 75, No. 5, pp. 1415–1419, 2009

0360-3016/09/$–see front matter

doi:10.1016/j.ijrobp.2008.12.063

CLINICAL INVESTIGATION **Brain**

STEREOTACTIC RADIOTHERAPY FOR INTRACRANIAL NONACOUSTIC SCHWANNOMAS INCLUDING FACIAL NERVE SCHWANNOMA

KENTARO NISHIOKA, M.D.,* DAISUKE ABO, M.D.,* HIDEFUMI AOYAMA, M.D.,* YASUSHI FURUTA, M.D.,† RIKIYA ONIMARU, M.D.,* SHUNSUKE ONODERA, M.D.,* YUTAKA SAWAMURA, M.D.,‡ MASAYORI ISHIKAWA, PH.D.,§ SATOSHI FUKUDA, M.D.,† AND HIROKI SHIRATO, M.D.*

Departments of *Radiology, †Oto-laryngology, ‡Neuro-surgery, and §Medical Physics, Graduate School of Medicine, Hokkaido University, Sapporo, Japan

Purpose: Although the effectiveness of stereotactic radiosurgery for nonacoustic schwannomas is currently being assessed, there have been few studies on the efficacy of stereotactic radiotherapy (SRT) for these tumors. We investigated the long-term outcome of SRT for nonacoustic intracranial nerve schwannomas.

Methods and Materials: Seventeen patients were treated between July 1994 and December 2006. Of these patients, 7 had schwannomas located in the jugular foramen, 5 in the trigeminal nerve, 4 in the facial nerve, and 1 in the oculomotor nerve. Radiotherapy was used as an initial treatment without surgery in 10 patients (59%) and after initial subtotal resection in the remaining patients. The tumor volume ranged from 0.3 to 31.3 mL (mean, 8.2 mL). The treatment dose was 40 to 54 Gy in 20 to 26 fractions. The median follow-up period was 59.5 months (range, 7.4–122.6 months). Local control was defined as stable or decreased tumor size on follow-up magnetic resonance imaging.

Results: Tumor size was decreased in 3 patients, stable in 13, and increased in 1 after SRT. Regarding neurologic symptoms, 8 patients (47%) had improvement and 9 patients were unchanged. One patient had an increase in tumor size and received microsurgical resection at 32 months after irradiation. No patient had worsening of pre-existing neurologic symptoms or development of new cranial nerve deficits at the last follow-up.

Conclusions: SRT is an effective alternative to surgical resection for patients with nonacoustic intracranial nerve schwannomas with respect to not only long-term local tumor control but also neuro-functional preservation.

Stereotactic radiotherapy, Facial nerve, Trigeminal nerve, Schwannoma.

INTRODUCTION

Schwannomas of the intracranial nerves account for about 10% of all brain tumors, and they are generated in the eighth nerve in about 90% of cases. Nonacoustic intracranial nerve schwannomas arise from the trigeminal nerve (V) in 0.8% to 8% of cases (1, 2), the jugular foramen (IX/X/XI) in 2.9% to 4% (3, 4), and the facial nerve (VII) in 1.9% (5, 6).

The standard treatment has been total removal via microsurgery. However, surgical total resection is often associated with the development of new neurologic deficits, and incomplete resection often results in tumor regrowth, which requires additional therapy. Sarma *et al.* (7) reported their experience with microsurgery in 46 cases of nonacoustic nerve schwannomas (trigeminal nerve in 26, jugular foramen in 9, facial nerve in 7, hypoglossal nerve in 3, and trochlear nerve in 1). They found that new cranial nerve deficit developed after surgery in 11 patients (24%), cerebrospinal fluid leaks in 5 (11%), meningitis in 3 (7%), and vasospasm requiring angioplasty in 1 (2%), with temporary hemiparesis in 2 cases and permanent hemiparesis in 1 case. Of the patients, 5 (28%) had improvement in pre-existing neurologic deficit.

On the basis of the effectiveness of radiation therapy for acoustic schwannomas, stereotactic radiosurgery (SRS) with a Gamma Knife or linear accelerator–based system has been applied to nonacoustic schwannomas, and an excellent local control rate and few adverse effects have been reported (8–14). Pollock *et al.* (8) administered SRS (12–20 Gy; mean tumor volume, 8.9 mL [range, 0.2–17.6 mL]) with a Gamma Knife to 23 patients (trigeminal nerve in 10, jugular foramen in 10, hypoglossal nerve in 2, and trochlear nerve in 1). The local control rate was 96% during the follow-up period (median, 43 months; range, 12–111 months), and new neurologic deficits developed in 3 cases (12%). Mabanta *et al.* (9) reported on 18 patients (trigeminal nerve in 7, jugular foramen in 9, and facial nerve in 2) who were treated

Reprint requests to: Hiroki Shirato, M.D., Department of Radiology, Graduate School of Medicine, Hokkaido University, North-15 West-7, Kita-ku, Sapporo, Japan, 060-0838. Tel: (+81) 11-706-5974; Fax: (+81) 11-706-7876; E-mail: shirato@med.hokudai.ac.jp

Conflict of interest: none.

Received Aug 21, 2008, and in revised form Dec 31, 2008. Accepted for publication Dec 31, 2008.

with linear accelerator radiosurgery (10–15 Gy; mean tumor volume, 5.5 mL [range, 0.7–15.4 mL]). The rate of tumor control was 100%, with worsening of pre-existing nerve VII palsy in 1 case and new-onset hearing loss in 2 cases.

Recent advances in image-guided radiotherapy have made it possible to use fractionated radiotherapy with stereotactic accuracy. Acoustic schwannomas are known to be well treated with fractionated stereotactic radiotherapy (SRT), and there is a lower rate of late adverse effects with this method than with SRS (15). Considering that acoustic schwannomas are often treated with SRT rather than SRS because of the expectation of reducing the late adverse effects, patients with nonacoustic schwannomas such as facial nerve schwannomas would be good candidates for SRT.

Supported by our experience with acoustic schwannomas (15, 16), we have performed SRT for nonacoustic intracranial nerve schwannomas since 1994. In this study we assessed the outcomes of SRT for patients with nonacoustic intracranial nerve schwannomas who were treated at our institution. To our knowledge, this is the largest series to date on the use of SRT for nonacoustic intracranial schwannoma.

METHODS AND MATERIALS

Between July 1994 and December 2006, 17 patients with nonacoustic intracranial nerve schwannomas were treated with SRT at our institution. There were 7 men and 10 women. The median age was 47 years (range, 20–75 years). Of the patients, 5 had schwannomas of the trigeminal nerve (V), 7 of the lower cranial nerves (IX/X/XI) (so-called jugular foramen schwannomas), 4 of the facial nerve (VII), and 1 of the oculomotor nerve (III). There was no patient who was diagnosed with neurofibromatosis.

The tumor volume at the start of radiotherapy ranged from 0.3 to 31.3 mL (mean, 8.2 mL). Surgical total resection had been performed as the initial treatment until 2000, but starting in April 2000, SRT was selected as the initial treatment in principle regardless of tumor size, site, age, and so on, because the effectiveness of SRT for intracranial schwannomas was gradually being clarified. Only 1 patient, who received SRT at December, 2006, had been initially treated by surgery at December, 1987. Of 17 patients, 6 had surgical resection as the initial treatment and radiotherapy was administered for residual or relapsed tumors. One patient had received craniotomy and biopsy before radiotherapy. Consequently, the period between surgery and radiotherapy varied from 0.9 to 228.2 months (median, 7.3 months).

The median total dose was 50 Gy (range, 40–54 Gy) given in 25 fractions in 6 weeks. Radiotherapy was administered 4 days per week with 2 Gy per fraction by use of a thermoplastic fixation device in principle. The fraction size was changed when the stereotactic boost was administered described as follows: One patient received an additional irradiation of 4 Gy in 1 fraction after 44 Gy in 22 fractions and two patients received 10 Gy in 4 fractions after 44 Gy in 22 fractions as a stereotactic boost at the end of the schedule via a direct traumatic fixation device (16).

The treatment planning was based on thin-slice computed tomography (CT) scans. Since October 1998, we have used magnetic resonance imaging (MRI) for planning in addition to CT scan. Five patients in the initial stage were treated without the use of MRI. The images from MRI and CT were overlapped on the computer, and the outline of the target and the organs at risk was enclosed. In principle, the clinical target volume margin was 1 mm and the planning target volume margin was 2 mm. The margin had been slightly modified by the therapeutic radiologist's judgement according to the tumor size, location, and surgical findings. The prescribed dose was given at the isocenter, and the planning target volume was covered by 80% to 90% of the prescribed dose. Conformity indices were not commonly used in the 1990s and were not able to be analyzed in this study. Three-dimensional treatment planning was performed by use of FOCUS and XiO systems (CMS Inc., Maryland Heights, MO).

Informed consent was obtained from all patients. Local tumor control was defined as stable or decreased tumor size on follow-up MRI after the last day of radiotherapy. The tumor volume was measured by use of contrast-enhanced T1-weighted MRI images.

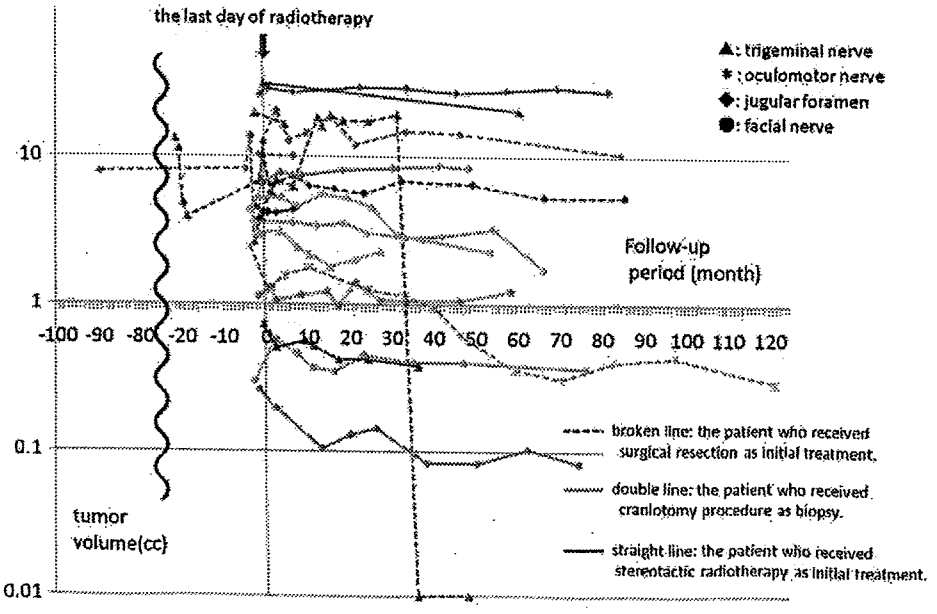

Fig. 1. Transition of tumor volume before and after stereotactic radiotherapy.

RESULTS

The median follow-up period was 59.5 months (range, 7.4–122.6 months). The local control rate was 94% (16 of 17 patients) at the last follow-up. The tumor size remained stable in 13 patients and decreased in 3 patients (Fig. 1). No obvious difference was observed between the patients who received radiotherapy after surgery and those initially treated by radiotherapy with respect to both local control and improvement of neurologic symptoms: 85.7% (6 of 7) versus 100% (10 of 10) and 57.1% (4 of 7) versus 50% (5 of 10), respectively. Tumor enlargement with cystic change was seen 12 months after SRT in 1 patient who received 44 Gy in 22 fractions plus 10 Gy in 4 fractions for postoperative recurrence of trigeminal nerve schwannoma. This patient received a salvage operation because the tumor had not decreased in size even at 32 months after SRT. The surgical specimen showed schwannoma cells and cysts with a wall of collagen fiber without evidence of gliosis. There was no relapse after the salvage surgery until she died of gastric carcinoma 92 months after surgery.

Regarding pre-existing neurologic symptoms, 8 of 17 patients (47%) improved and 9 patients remained unchanged. Among the 4 patients with facial nerve schwannomas, none had worsening of their pre-existing neurologic symptoms and 2 patients showed an improvement (Table 1). Temporary nausea, taste change, dizziness, tinnitus, and headache were seen in 5 patient, 3 patients, 2 patients, 1 patient, and 1 patient, respectively. All these patients showed improvement during the follow-up period. No patients had new cranial nerve deficit or other symptomatic adverse effects develop. Intracranial malignant tumor did not develop any patient, suggesting that there was no radiation-induced secondary carcinogenesis during the follow-up period.

DISCUSSION

Stereotactic irradiation by use of precise diagnostic images and accurate fixation has been proven useful to treat intracranial benign tumors. Fractionated radiotherapy is expected to reduce the risk of injury to the surrounding normal structures and to better preserve normal tissue function than single-dose irradiation. It has been reported that SRT is superior to SRS with regard to the preservation of acoustic function (17, 18), and the same may be true for nonacoustic intracranial schwannomas. Fractionated SRT has also been suggested to be more effective for cystic-type schwannomas than SRS (19). In addition, the fractionated radiotherapy does not require an invasive fixation and is more comfortable for the patients than SRS, with the only requirement being that patients are available to visit the clinic frequently.

Zabel *et al.* (20) administered SRT (total dose of 54–57.6 Gy, 5 days per week, with 1.8 Gy per fraction) for 13 nonacoustic intracranial schwannomas (located in the trigeminal nerve in 7 cases, located in the lower cranial nerve origin in 3, and located in the cerebellopontine angle without involvement of the acoustic nerve in 3) from 1996 to 2000. They found that the local control rate was 100% and there was no development of new cranial nerve or brain stem deficits over the median follow-up period of 33 months (range, 13–70 months). Improvement of pre-existing neurologic deficit was seen in 4 patients (31%). The authors concluded that SRT is an effective and well-tolerated noninvasive treatment for nonacoustic intracranial schwannoma, with an excellent tumor control rate.

Our study showed that the local control rate of SRT was 94% (16 of 17 patients) after a median imaging follow-up of 59.5 months. The mean tumor volume was 8.2 mL with a range of 0.3 to 31.3 mL, which is equivalent to the values in the

Table 1. Characteristics of patients with facial nerve schwannoma

Patient no.	Gender	Age (y)	Side	Surgery	Size (mm)	Dose (Gy/ fractions/d)	Follow-up (mo)	Tumor size	Symptoms	Adverse effect
6	F	25	Right	None	13 × 13 × 15	50/25/51	61.8	No remarkable change (14 × 13 × 13)	Grade II facial palsy; unchanged after SRT	None
9	F	20	Left	None	9 × 8 × 8	50/25/49	77.7	No remarkable change (11 × 8 × 8)	Grade II facial palsy; subjectively improved after SRT	None
10	F	43	Left	None	5 × 5 × 20	50/25/45	75.7	Decreased (4 × 4 × 10)	Grade II facial palsy; subjectively improved after SRT	None
13	M	26	Right	None	22 × 19 × 20	50/25/45	54.0	Decreased (21 × 15 × 14)	Grade IV facial palsy; unchanged after SRT	Temporal nausea and headache

Abbreviations: F = female; SRT, stereotactic radiotherapy; M = male.

Table 2. Surgical resection, stereotactic radiosurgery, and stereotactic radiotherapy for nonacoustic schwannomas

Series	No. of patients	Tumor size	Follow-up	Local control	Neurologic deficits (patients)	Neurologic improvement (patients)
Surgical resection						
Sarma *et al.* (7), 2002	46 (V in 26, VII in 7, IX/X/XI in 9, XII in 3, III in 1)	N.R.	Mean, 33.6 mo	100%	New deficits in 11 (24%)	II in 4, III in 5, IV in 2, V in 9, VI in 9, VII in 6, VIII in 6, IX/X/XI in 4
Samii *et al.* (1, 3), 1995	12 (V)	From 2 × 2 × 3 cm to 4 × 4 × 5 cm	Mean, 25 mo	83%	Temporary paraparesis in 1, temporary facial weakness in 2	N.R.
	16 (IX/X/XI)	From 1 × 1 cm to 6 × 5 cm	Mean, 22 mo	100%	Temporary cranial nerve morbidity in 6 (38%), new deficits in 11 (50%)	N.R.
Sanna *et al.* (10), 2006	22 (IX/X/XI)	N.R.	Mean, 36.6 mo	100%	Worsened VII in 3, VIII in 2	VII in 1, VIII in 2
Day and Fukushima (21), 1998	38 (V)	N.R.	Mean, 77 mo	97%	New or worsened V in 53%	Diplopia in 4, headache in 5, ataxia in 2
Stereotactic radiosurgery						
Pollock *et al.* (8), 2002	23 (V in 10, IX/X/XI in 10, XII in 2, IV in 1)	Median prescription isodose volume, 8.9 mL	Median, 43 mo	96%	New or worsened V in 3 (10%)	N.R.
Mabanta *et al.* (9), 1999	18 (V in 7, VII in 2, IX/X/XI in 9)	Mean volume, 5.5 mL	Mean, 32 mo	100%	Worsening of pre-existing VII palsy in 1 (6%), new onset of hearing loss in 2 (11%)	5 (28%)
Kida *et al.* (5), 2007	14 (VII)	Mean volume, 5.5 mL	Mean, 31.4 mo	100%	Worsened VII in 1 (7%)	5 (36%)
Litre *et al.* (11), 2007	11 (VII)	Mean volume, 0.888 mL	Median, 39 mo	91%	Did not worsen in any patient	VII in 3 (27%), balance problems and hearing in 1 (9%)
Huang *et al.* (12), 1999	16 (V)	Mean volume, 5.3 mL	Mean, 44 mo	100%	Did not observe any new neurologic deficits	5 (31%)
Martin *et al.* (13), 2007	34 (IX/X/XI)	Median, 4.2 mL	Mean, 83 mo	94%	Worsened in 1 (3%)	20% of affected cranial nerves
Muthukumar *et al.* (14), 1999	17 (IX/X/XI)	Median tumor diameter, 22.5 mm	Median, 39 mo	94%	Worsened in 1 (8%)	6 (46%)
Stereotactic radiotherapy						
Wallner *et al.* (22), 1988	18	N.R.	Range, 2–15 y	50%	N.R.	N.R.
Zabel *et al.* (20), 2001	13 (V in 7, lower cranial nerve in 3, cerebellopontine angle in 3)	Median, 19.8 mL	Median, 33 mo	100%	Slight worsening of pre-existing V/XII in 1 (8%)	4 (31%)
Present series	17 (V in 5, IX/X/XI in 7, VII in 4, III in 1)	Mean, 8.2 mL	Median, 59.5 mo	94%	No patient had development of new neurologic deficit	8 (47%)

Abbreviations: V = trigeminal nerve; VII = facial nerve; IX/X/XI = glossopharyngeal nerve/vagus nerve/accessory nerve passing through jugular foramen; XII = hypoglossal nerve; III = oculomotor nerve; N.R. = not reported; II = optic nerve; IV = trochlear nerve; VI = abducent nerve; VIII = vestibulocochlear nerve.

previous series using SRS (8–14) and SRT (20). No patient showed a worsening of pre-existing neurologic symptoms or had new cranial nerve deficits develop. Improvement of pre-existing neurologic symptoms was seen in 8 patients (47%), which is a relatively high rate in comparison to existing reports (Table 2). No severe complications were observed during

follow-up. In clinical practice facial nerve schwannoma has probably been the most harmful disease among the nonacoustic intracranial schwannomas because of the facial nerve palsy after total resection. However, it was notable that in our series no patients had worsening of their pre-existing neurologic symptoms and 2 patients showed an improvement. Mabanta *et al.* (9) reported that SRS achieved local control of 2 facial nerve schwannomas, although one of these cases had worsening of pre-existing facial nerve palsy. Considering that worsening of facial palsy often induces depression in patients and reduces their quality of life, SRT should be considered an alternative to surgery for patients with facial nerve schwannoma. SRT is at least as effective as SRS and possibly more effective in preserving neurologic function, although the number of patients is too small to compare between SRT and SRS for nonacoustic intracranial schwannoma.

Transient enlargement of schwannoma with cystic change is often seen in patients with acoustic schwannoma (19), but little is known about the phenomenon of nonacoustic schwannoma. We have seen 1 patient with a trigeminal nerve schwannoma who had enlargement of the tumor with cystic change for as long as 32 months after SRT. Considering that cystic enlargement of acoustic schwannomas is usually transient, there might be a difference between acoustic and nonacoustic intracranial schwannomas with respect to the ability to resolve the cystic degeneration, although the number of patients in this study was too small to reach a conclusion on this matter.

The optimal radiation dose for the nonacoustic intracranial schwannoma is not known. At our institution, we initially used 4 Gy in 1 fraction or 10 Gy in 4 fractions as a stereotactic boost, but its clinical efficacy was not certain. Fifty grays in 25 fractions, which is used for acoustic schwannoma, would be a reasonable dose for nonacoustic intracranial schwannoma as well.

In conclusion, although the number of patients in each group (*i.e.*, different anatomic sites and treatment methods) is small because of the rarity of nonacoustic intracranial schwannomas, SRT can provide long-term tumor control with a low incidence of neurologic complications for nonacoustic intracranial schwannomas, including facial nerve schwannomas.

REFERENCES

1. Samii M, Migliori MM, Tatagiba M, *et al.* Surgical treatment of trigeminal schwannomas. *J Neurosurg* 1995;82:711–718.
2. Konovalov AN, Spallone A, Mukhamedjanov DJ, *et al.* Trigeminal neurinomas. A series of 111 surgical cases from a single institution. *Acta Neurochir (Wien)* 1996;138:1027–1035.
3. Samii M, Babu RP, Tatagiba M, *et al.* Surgical treatment of jugular foramen schwannomas. *J Neurosurg* 1995;82:924–932.
4. Tan LC, Bordi L, Symon L, *et al.* Jugular foramen neuromas: A review of 14 cases. *Surg Neurol* 1990;34:205–211.
5. Kida Y, Yoshimoto M, Hasegawa T. Radiosurgery for facial schwannomas. *J Neurosurg* 2007;106:24–29.
6. Symon L, Cheesman AD, Kawauchi M, *et al.* Neuromas of the facial nerve: A report of 12 cases. *Br J Neurosurg* 1993;7: 13–22.
7. Sarma S, Sekhar LN, Schessel DA. Nonvestibular schwannomas of the brain: A 7-year experience. *Neurosurgery* 2002;50: 437–449.
8. Pollock BE, Foote RL, Stafford SL. Stereotactic radiosurgery: The preferred management for patients with nonvestibular schwannomas? *Int J Radiat Oncol Biol Phys* 2002;52: 1002–1007.
9. Mabanta SR, Buatti JM, Friedman WA, *et al.* Linear accelerator radiosurgery for nonacoustic schwannomas. *Int J Radiat Oncol Biol Phys* 1999;43:545–548.
10. Sanna M, Bacciu A, Falcioni M, *et al.* Surgical management of jugular foramen schwannomas with hearing and facial nerve function preservation: A series of 23 cases and review of the literature. *Laryngoscope* 2006;116:2191–2204.
11. Litre CF, Gourg GP, Tamura M, *et al.* Gamma knife surgery for facial nerve schwannomas. *Neurosurgery* 2007;60:853–859.
12. Huang C-F, Kondziolka D, Flickinger JC, *et al.* Stereotactic radiosurgery for trigeminal schwannomas. *Neurosurgery* 1999; 45:11–16.
13. Martin JJ, Kondziolka D, Flickinger JC, *et al.* Cranial nerve preservation and outcome after stereotactic radiosurgery for jugular foramen schwannomas. *Neurosurgery* 2007;61:76–81.
14. Muthukumar N, Kondziolka D, Lunsford LD, *et al.* Stereotactic radiosurgery for jugular foramen schwannomas. *Surg Neurol* 1999;52:172–179.
15. Shirato H, Sakamoto T, Sawamura Y, *et al.* Comparison between observation policy and fractionated stereotactic radiotherapy (SRT) as an initial management for vestibular schwannoma. *Int J Radiat Oncol Biol Phys* 1999;44:545–550.
16. Kagei K, Shirato H, Suzuki K, *et al.* Small-field fractionated radiotherapy with or without stereotactic boost for vestibular schwannoma. *Radiother Oncol* 1999;50:341–347.
17. Fuss M, Debus J, Lohr F, *et al.* Conventionally fractionated stereotactic radiotherapy (FSRT) for acoustic neuromas. *Int J Radiat Oncol Biol Phys* 2000;48:1381–1387.
18. Andrews DW, Suarez O, Goldman HW, *et al.* Stereotactic radiosurgery and fractionated stereotactic radiotherapy for the treatment of acoustic schwannomas. Comparative observation of 125 patients treated at one institution. *Int J Radiat Oncol Biol Phys* 2001;50:1265–1278.
19. Shirato H, Sakamoto T, Takeichi N, *et al.* Fractionated stereotactic radiotherapy for vestibular schwannoma (VS): Comparison between cystic-type and solid-type VS. *Int J Radiat Oncol Biol Phys* 2000;48:1395–1401.
20. Zabel A, Debus J, Thilmann C, *et al.* Management of benign cranial nonacoustic schwannomas by fractionated stereotactic radiotherapy. *Int J Cancer* 2001;96:356–362.
21. Day JD, Fukushima T. The surgical management of trigeminal neuromas. *Neurosurgery* 1998;42:233–241.
22. Wallner KE, Pitts LH, Davis RL, *et al.* Radiation therapy for the treatment of non-eighth nerve intracranial neurilemmoma. *Int J Radiat Oncol Biol Phys* 1988;14:287–290.

Original Article | DOI 10.3349/ymj.2010.51.1.93 pISSN: 0513-5796, eISSN: 1976-2437 | Yonsei Med J 51(1): 93-99, 2010 | YMJ

High Dose Three-Dimensional Conformal Boost Using the Real-Time Tumor Tracking Radiotherapy System in Cervical Cancer Patients Unable to Receive Intracavitary Brachytherapy

Hee Chul Park,[1,2] Shinichi Shimizu,[1] Akio Yonesaka,[1] Kazuhiko Tsuchiya,[1] Yasuhiko Ebina,[3] Hiroshi Taguchi,[1] Norio Katoh,[1] Rumiko Kinoshita,[1] Masayori Ishikawa,[1] Noriaki Sakuragi,[3] and Hiroki Shirato[1]

Departments of [1]Radiology and [3]Gynecology, Hokkaido University Graduate School of Medicine, Sapporo, Japan; [2]Department of Radiation Oncology, Sungkyunkwan University School of Medicine, Samsung Medical Center, Seoul, Korea.

Purpose: The purpose of this study is to evaluate the clinical results of treatment with a high dose of 3-dimensional conformal boost (3DCB) using a real-time tracking radiation therapy (RTRT) system in cervical cancer patients. **Materials and Methods:** Between January 2001 and December 2004, 10 patients with cervical cancer were treated with a high dose 3DCB using RTRT system. Nine patients received whole pelvis radiation therapy (RT) with a median dose of 50 Gy (range, 40-50 Gy) before the 3DCB. The median dose of the 3DCB was 30 Gy (range, 25-30 Gy). Eight patients received the 3DCB twice a week with a daily fraction of 5 Gy. The determined endpoints were tumor response, overall survival, local failure free survival, and distant metastasis free survival. The duration of survival was calculated from the time of the start of radiotherapy. **Results:** All patients were alive at the time of analysis and the median follow-up was 17.6 months (range, 4.9-27.3 months). Complete response was achieved in nine patients and one patient had a partial response. The 1- and 2-year local failure free survival was 78.8% and 54%, respectively. The 1- and 2-year distant metastasis free survival was 90% and 72%, respectively. Late toxicity of a grade 2 rectal hemorrhage was seen in one patient. A subcutaneous abscess was encountered in one patient. **Conclusion:** The use of the high dose 3DCB in the treatment of cervical cancer is safe and feasible where intracavitary brachytherapy (ICBT) is unable to be performed. The escalation of the 3DCB dose is currently under evaluation.

Key Words: Uterine cervical neoplasms, radiotherapy, brachytherapy

Received: December 1, 2008
Revised: February 26, 2009
Accepted: April 8, 2009
Corresponding author: Dr. Hiroki Shirato, Department of Radiology, Hokkaido University Graduate School of Medicine, North-15 West-7, Sapporo 060-8638, Japan.
Tel: 81-11-706-7676, Fax: 81-11-706-5975
E-mail: shirato@med.hokudai.ac.jp

The authors have no financial conflicts of interest.

INTRODUCTION

Intracavitary brachytherapy (ICBT) in combination with external-beam radiotherapy (EBRT) has long been accepted as the standard treatment for uterine cervical cancer.[1] ICBT is used to deliver high radiation doses to the clinical target volume (CTV) by replacing radioactive sources that are in direct contact with the gross tumor. Traditionally, it is known that a cure is rarely achieved without a high dose of radiation delivered by ICBT. However, the clinical reality is that the treatment with EBRT alone is needed in patients where ICBT is not feasible due to a failure to insert a tandem, a narrow vagina, relapses at the cervical stump, or the refusal of the patient. Interstitial brachytherapy is often helpful in these cases, but it involves invasive procedures and its success is highly dependent on the

ability of the operator.[2]

Replacing the use of ICBT with an EBRT boost should be applicable with the advances of the conformal radiation delivery technique. Some innovative researchers have challenged the use of ICBT by using EBRT instead with modest results obtained.[3-8] However, in these studies, severe complications were observed in some patients. While the use of ICBT can keep a fixed geometry between the CTV and the applicator, minimizing the error in delivering the planned dose distribution to the target, EBRT has shortcomings with regards to setup errors and possible internal organ motion. To overcome these shortcomings, a fluoroscopic real-time tumor tracking radiotherapy (RTRT) system was developed and applied for the treatment of pelvic malignancies.[9-11] We have previously reported the feasibility and accuracy of the use of a high dose three-dimensional conformal boost (3DCB) with the RTRT system in patients with gynecologic malignancies.[12] The RTRT system was useful to reduce the uncertainty due to external and internal error, confirming that a planning target volume (PTV) margin of 7-8 mm should be applied in the protocol setting.

To maintain similar therapy conditions to the tumor as with ICBT, the daily dose and the overall treatment time with the use of a high dose 3DCB are needed to be kept similar as with ICBT. The usual fractionation scheme for ICBT in our institution was 25 Gy/5 fractions or 35 Gy/7 fractions, with a daily fraction of 5 Gy and two fractions per week.[13] Using the RTRT technology, we applied a hypofractionated 3DCB mimicking ICBT in patients with uterine cervical cancer that were unable to undergo ICBT after EBRT.

In this report, early clinical results of cervical cancer patients treated with high dose 3DCB using the RTRT system were evaluated. The possibility of high precision conformal therapy using the RTRT technology as an alternative to ICBT is discussed.

MATERIALS AND METHODS

Patients

Between January 2001 and December 2004, 10 patients with cervical cancer were treated with a high dose 3DCB using the RTRT system without ICBT. Before starting the 3DCB, we explained to the patients that the standard definitive radiotherapy (RT) method was a combination of EBRT and ICBT, but the use of a high dose 3DCB with the RTRT system could be an option in patients unable to undergo ICBT. All patients decided to receive a high dose 3DCB. Pre-treatment evaluation included a complete history and physical examination, biopsy, abdominal and pelvic computed tomography (CT), and chest X-ray. Lymph node sampling was not performed routinely. Threshold value for identifying metastatic LNs was 10 mm short axis diameter. Patients with an outside pathology diagnosis had their pathology slides reviewed at our institution. For staging purposes, a radiation oncologist and a gynecologic oncologist performed a physical examination. Staging was performed according to the International Federation of Gynecology and Obstetrics (FIGO) classification.[14]

Five patients with newly diagnosed uterine cervical cancer, two patients with a stump carcinoma, and three patients with a vault recurrence were included in the analysis. Three patients with a vault recurrence received a radical hysterectomy due to FIGO stage I cervical cancer. Postoperative radiotherapy was added in 1 patient (patient 2). Two patients with a stump carcinoma received a hysterectomy due to myoma. The median age of the patients was 64 years (range, 32-78 years). The patient and tumor characteristics are summarized in Table 1.

Table 1. Characteristics of 10 LN (-) Patients

Patient number	Age (yrs)	KPS	Site	Histology	FIGO stage	Tumor size (cc)
1	32	90	Cervix	Small	IIB	80
2	65	90	Vault	Squamous	IIB	30
3	35	90	Cervix	Adenosarcoma	IIIB	192
4	70	80	Cervix	Squamous	IIIB	240
5	63	90	Vault	Squamous	IIB	24
6	69	80	Cervix	Squamous	IIIB	80
7	57	90	Vault	Squamous	IIIB	40
8	67	80	Cervix	Squamous	IIIB	64
9	60	90	Stump	Squamous	IIA	18
10	78	70	Stump	Squamous	IIA	20

LN, lymph node; KPS, Karnofsky performance score; FIGO, International Federation of Gynecology and Obstetrics; Small, small cell carcinoma; Squamous, squamous cell carcinoma.

Treatment planning and treatment

The general principles of treatment planning and delivery were reported in previous studies.[9-12] If ICBT and interstitial RT were abandoned and the patients agreed to enter this study, three radiopaque gold markers were implanted in or near the tumor by a trans-vaginal approach using specially made equipment (Medikit, Tokyo, Japan). After the gold markers were implanted, a planning CT scan was performed using a 1 mm slice thickness for the level involving the tumor mass and three gold markers (Fig. 1). The treatment planning was performed using the Focus® system (CMS, St. Louis, MO USA). The CTV encompassed the gross tumor volume with a safety margin. Usually, a safety margin of up to 5 mm was taken. In lateral directions, a safety margin of 8 mm was used. For the PTV, a 7-8 mm margin from the CTV was applied. After finishing the treatment planning, the coordinates of the target volume, isocenter, and three markers were registered and sent to the RTRT system. After adjusting the patient set-up using the RTRT system, the treatment was delivered. We checked the intrafractional movement of the marker several times during each treatment while the gantry was moving to the next position. The details of set-up and the radiation delivery procedure in our protocol setting were reported previously.[12]

Fig. 1. Fluoroscopy and planning CT image of three gold markers placed in a patient.

The treatment characteristics of the patients are summarized in Table 2. Nine patients received a whole pelvis RT with a median dose of 50 Gy (range, 40-50 Gy). Midline shielding was performed in six patients after a dose of 40 Gy. The median dose of the 3DCB was 30 Gy (range, 25-30 Gy). The 3DCB was delivered by a 3D-conformal technique (7 patients) and forward planning intensity-modulated radiation therapy (IMRT) technique (3 patients). Eight patients received the 3DCB twice a week with a daily fraction of 5 Gy, as with the ICBT fractionation scheme of our institution.[12] Two patients received 2.5 Gy daily fractions 3-4 times a week. The treatment volume typically covered the gross tumor and the area of parametrium invasion. Concurrent chemotherapy with weekly cisplatin was administered to three patients.

Follow-up

Patients were scheduled for follow-up visits every 3 months. We determined the dates of local and distant failure using imaging studies, primarily abdomen and pelvic CT scans, which were performed at approximately three-month intervals during the initial two years of follow-up.

End points and statistical analysis

The major endpoints of this study were tumor response, overall survival (OS), local failure free survival (local failure, defined as any recurrence within the RT volume), and distant metastasis free survival. Nodal recurrences were also evaluated. Late toxicity was graded according to the Radiation Therapy Oncology Group/European Organization for Research and Treatment of Cancer late radiation

Table 2. Treatment Characteristics of the Patients

Patient number	Pelvis dose (Gy)	Midline shielding at (Gy)	3DCB dose (Gy)	3DCB fraction size (Gy)	3DCB fractionation (number/weekly)	3DCB technique	Concurrent CTX
1	50	40	30	5	2	3DCRT	Yes
2	0	-	30	2.5	3	3DCRT	-
3	50	40	25	2.5	4	3DCRT	Yes
4	50	40	30	5	2	FIMRT	-
5	50	40	30	5	2	3DCRT	-
6	50	-	30	5	2	3DCRT	-
7	50	40	30	5	2	FIMRT	-
8	50	-	30	5	2	FIMRT	Yes
9	50	-	30	5	2	3DCRT	-
10	40	-	30	5	2	3DCRT	-

3DCB, 3-dimensional conformal boost; 3DCRT, 3-dimentional conformal radiation therapy; FIMRT, forward planning intensity-modulated radiation therapy; CTX, chemotherapy.

morbidity scoring scheme.[15]

The duration of the follow-up period was calculated from the date of the first visit to our clinic. The duration of survival was calculated from the day of commencing RT. The survival time was censored at the time of the last follow-up on record if death was not observed. Dates of local and distant failure were determined using imaging studies. Survival probabilities were estimated non-parametrically using the Kaplan-Meier's product limit method.[16]

RESULTS

Clinical response

The endpoints are summarized in Table 3. Of 10 patients, complete response (CR) of the tumor was achieved in nine patients (90%), and one patient had a partial response (PR). Therefore, the response rate (CR + PR) was 100%. Fig. 2 shows the tumor response in case 5.

Disease control and survival

All patients were still alive at the time of analysis and the median follow-up was 17.6 months (range 4.9-27.3 months) (Fig. 3). Four patients were alive without disease, and six patients were alive with disease. Four patients had local failure and the crude rate of local control was 60%. Two patients had distant metastases and the crude rate of distant disease control was 80%. One patient had a liver and bone metastasis and the other patient had a metastasis to the para-aortic lymph node and the adrenal gland. The actuarial 1 year and 2 year local failure free survival was 78.8% and 54%, respectively. The actuarial 1 year and 2 year distant metastasis free survival was 90% and 72%, respectively.

Treatment toxicities

All patients tolerated the 3DCB very well and no severe adverse effects were encountered. However, acute toxicity of grade 1 diarrhea was seen in five patients. Late toxicity of grade 2 rectal hemorrhage was seen in one patient. A subcutaneous abscess was encountered in one patient 6 months after the completion of RT.

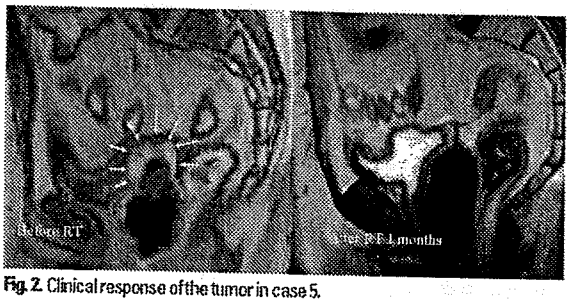

Fig. 2. Clinical response of the tumor in case 5.

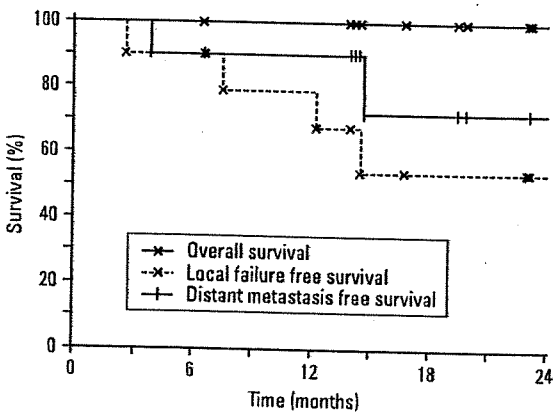

Fig. 3. Survival plotting.

Table 3. Summary of the Treatment Results

Patient number	Tumor response	Local recurrence	Distant metastasis	Complications	FU periods (months)	Current status
1	CR	-	Liver, bone	G2 rectal	16.9	AWD
2	CR	-	-	-	23.7	NED
3	PR	Y	-	-	21.0	AWD
4	CR	Y	-	-	18.2	AWD
5	CR	-	-	-	27.3	NED
6	CR	-	-	Subcutaneous abscess	12.5	NED
7	CR	Y	-	-	14.9	AWD
8	CR	-	PA node, adrenal gland	-	21.7	AWD
9	CR	Y	-	-	12.5	AWD
10	CR	-	-	-	5.0	NED

FU, follow-up; CR, complete response; PR, partial response; Y, yes; PA, para-aortic; G, grade; AWD, alive with disease; NED, no evidence of disease.

DISCUSSION

It is well known that ICBT is an essential component of RT for uterine cervical cancer.[1] With a direct contact to the tumor, ICBT effectively delivers the tumoricidal dose while sparing the surrounding normal tissue. However, a small but definite proportion of patients are not suitable to undergo ICBT for several clinical reasons. Thus, we intended to treat those patients with a high dose 3DCB replacing the ICBT portion of the entire treatment. The RTRT technology provides the effective tools to realize individual-based, precise adaptive irradiation for moving, shrinking, and deforming targets, such as gynecologic malignancies. In an effort to mimic the ICBT portion of the treatment, we applied RTRT technology in the current protocol settings.

The treatment results of the use of the high dose 3DCB in the present study were not satisfying. The local failure free survival was relatively low at 2 years. Though there were six patients with disease recurrence, the OS was still 100% because of the short-term follow-up. It is thought that a further follow-up with more patients could confirm the treatment results and the effectiveness of our study protocol. In our study, the adaptive set-up of patients using the RTRT system was proved as a safe adjunct showing a minimal level of late complications. It seems that further escalation of the 3DCB dose could be pursued safely. Among patients with local failure, three patients had FIGO IIIB disease and two patients had a large tumor size (patient 3 and 4). The escalation of the 3DCB dose is being evaluated to improve local control for these patients with locally advanced diseases.

Some investigators have performed definitive external radiation therapy without ICBT for uterine cervical cancer.[3,4,6] Table 4 shows the treatment results of these studies. Matsuura, et al.[3] used concomitant boost with accelerated hyperfractionation to shorten the overall treatment time as compared to ICBT. However, due to a small study population and short term follow-up, the level of local control (85.7%) and survival comparable to the results of standard treatment has not yet been confirmed. The particle radiation therapy series has shown better long-term local control and survival.[4,6] However, these studies showed a significant level of late morbidity. Detrimental set-up errors and internal organ motion contributed to late morbidity resulting from a high dose to the surrounding normal tissues. The use of a better adaptive set-up strategy is needed for the successful execution of definitive EBRT for gynecologic malignancies.

Except in the clinical situation in which proper ICBT cannot be performed, the use of ICBT is being challenged in many studies. Several researchers have performed a dosimetric comparison between the use of IMRT and ICBT in terms of dose homogeneity and target coverage.[17-20] Chan, et al.[21] compared different EBRT techniques as an alternative to ICBT. These investigators showed that the use of IMRT could improve target coverage and reduce the dose to critical structures. Moreover, when used in conjunction with a suitable immobilization system, IMRT may provide an alternative to ICBT. The average minimum tumor dose was significantly greater and the mean percent tumor volume receiving more than the prescription dose was higher with IMRT. The mean volume at the tolerance limit decreased for the bladder. These advantages of IMRT

Table 4. Outcomes for Various Studies Evaluating the Role of EBRT to Replace ICBT

Author (yr)	Patients (No.)	FIGO Stage	Treatment	Local control	Survival	Complication
Kagei, et al.[6]	25	IIB - IVA	Photon + Proton beam therapy Pelvis with X-ray 50.4 Gy / 28 Fx Tumor boost 37 - 101 Gy	75% (5 yr)	59% (10 yr)	24% grade 2 - 4 GI complication 8% grade 2 - 4 complication
Kato, et al.[4]	44	IIIB - IVA	Carbon ion radiotherapy Pelvis 35.2 - 44.8 GyE Tumor Boost 24 - 28 GyE	45 - 79% (5 yr)	37 - 43% (5 yr)	25% Grade 2 - 4 GI complication 9.1% Grade 2 GU complication
Matsuura, et al.[3]	7	IB - IVA	Concomittant boost AHF Pelvis 45 Gy / 25 Fx Tumor boost 21 - 28 Gy / 15 Fx	85.7% (2 yr)	85.7% (2 yr)	28.6% Grade 2 rectal complication
Present study	10	IIA - IIIB	High dose 3DCB using RTRT Pelvis 40 - 50 Gy / 20 - 25 Fx Tumor boost 30 Gy / 6 Fx	54% (2 yr)	72% (2 yr)	10% Grade 2 rectal complication 10% Subcutaneous abscess

EBRT, external beam radiation therapy; ICBT, intracavitary brachytherapy; FIGO, International Federation of Gynecology and Obstetrics; Fx, fractions; Gy, gray; GyE, gray equivalent; AHF, accelerated hyperfractionation; 3DCB, 3-dimensional conformal boost; RTRT, real-time tracking radiotherapy; GI, gastrointestinal; GU, genitourinary.

over ICBT are accentuated, especially in large volume tumors.

A weakness of ICBT is that tumors may have a particular size or geometry that places much of the tumor volume in peripheral under-dosed regions. Furthermore, critical structures may be over-dosed because of their proximity to the radioactive sources. To optimize the ICBT planning at best, some recommendations have been published on the use of 3-dimensional image-based treatment planning in ICBT.[22-24] However, even with the best optimization, it seems that the weakness of ICBT could not be removed completely due to the interplay between the tumor shape and the limited degree of freedom of the applicator geometry. Chao, et al.[25] investigated the consequences of uterosacral space involvement in patients with stage IIIB cervical cancer. These investigators concluded that the combination of ICBT and EBRT did not deliver an adequate dose to the tumor in the uterosacral space, and an improved dose delivery regimen should be investigated.

Non-uniform doses are unavoidable in ICBT resulting in a hot spot and cold spot that develop in the tumor. This inhomogeneity in the dose delivered by the ICBT is both advantageous and disadvantageous for tumor control. Since a dose deficit to a 1% sub-volume of the target larger than 20% of the prescription dose may lead to serious loss of tumor control probability (TCP), even if 80% of the target receives a 10% boost, particular attention is required for small-volume cold regions in the target.[26] Once the target is covered adequately, the use of deliberate non-uniform doses may increase the TCP. Tome, et al.[26,27] reported that up to 30% of a sub-volume boost to the 60-80% of the target volume appeared worthwhile or necessary to maximize the TCP. IMRT gives the best scenario of inhomogeneous irradiation with adequate target coverage. The simultaneous integrated boost (SIB) technique of IMRT was successfully applied in the treatment of head and neck cancer.[28] Thus, IMRT using RTRT technology can be the best modality for EBRT to replace ICBT in the treatment of cervical cancer. We have reported the feasibility of the use of synchronized IMRT using the RTRT system. Unlike the thoracic and upper gastrointestinal malignancies in which a narrow gating window is needed, it is thought that this technique could be applied successfully in the treatment of pelvic malignancies without an excess fluoroscopy dose to the skin surface.[29]

In conclusion, although more patients with longer follow-up periods are needed to evaluate the usefulness of high dose 3DCB, especially to determine the long-term toxicity level, our results suggest that a high dose of 3DCB replacing ICBT in the treatment of gynecologic malignancies is safe and feasible where ICBT is unable to be performed. To improve local control, the escalation of the radiation dose should be pursued. The use of synchronized IMRT with the RTRT system is a promising therapy and needs to be investigated further.

ACKNOWLEDGEMENTS

This work was supported in part by a grant from the Japanese Ministry of Education, Culture, Sports, Science and Technology.

REFERENCES

1. Park HC, Suh CO, Kim GE. Fractionated high-dose-rate brachytherapy in the management of uterine cervical cancer. Yonsei Med J 2002;43:737-48.
2. Hughes-Davies L, Silver B, Kapp DS. Parametrial interstitial brachytherapy for advanced or recurrent pelvic malignancy: the Harvard/Stanford experience. Gynecol Oncol 1995;58:24-7.
3. Matsuura K, Tanimoto H, Fujita K, Hashimoto Y, Murakami Y, Kenjo M, et al. Early clinical outcomes of 3D-conformal radiotherapy using accelerated hyperfractionation without intracavitary brachytherapy for cervical cancer. Gynecol Oncol 2007;104:11-4.
4. Kato S, Ohno T, Tsujii H, Nakano T, Mizoe JE, Kamada T, et al. Dose escalation study of carbon ion radiotherapy for locally advanced carcinoma of the uterine cervix. Int J Radiat Oncol Biol Phys 2006;65:388-97.
5. Mollá M, Escude L, Nouet P, Popowski Y, Hidalgo A, Rouzaud M, et al. Fractionated stereotactic radiotherapy boost for gynecologic tumors: an alternative to brachytherapy? Int J Radiat Oncol Biol Phys 2005;62:118-24.
6. Kagei K, Tokuuye K, Okumura T, Ohara K, Shioyama Y, Sugahara S, et al. Long-term results of proton beam therapy for carcinoma of the uterine cervix. Int J Radiat Oncol Biol Phys 2003;55:1265-71.
7. Ulmer HU, Frischbier HJ. Treatment of advanced cancers of the cervix uteri with external irradiation alone. Int J Radiat Oncol Biol Phys 1983;9:809-12.
8. Castro JR, Issa P, Fletcher GH. Carcinoma of the cervix treated by external irradiation alone. Radiology 1970;95:163-6.
9. Shirato H, Shimizu S, Kunieda T, Kitamura K, van Herk M, Kagei K, et al. Physical aspects of a real-time tumor-tracking system for gated radiotherapy. Int J Radiat Oncol Biol Phys 2000;48:1187-95.
10. Kitamura K, Shirato H, Shinohara N, Harabayashi T, Onimaru R, Fujita K, et al. Reduction in acute morbidity using hypofractionated intensity-modulated radiation therapy assisted with a fluoroscopic real-time tumor-tracking system for prostate cancer: preliminary results of a phase I/II study. Cancer J 2003;9:268-76.
11. Shimizu S, Shirato H, Kitamura K, Shinohara N, Harabayashi T, Tsukamoto T, et al. Use of an implanted marker and real-time tracking of the marker for the positioning of prostate and bladder cancers. Int J Radiat Oncol Biol Phys 2000;48:1591-7.
12. Yamamoto R, Yonesaka A, Nishioka S, Watari H, Hashimoto T, Uchida D, et al. High dose three-dimensional conformal boost (3DCB) using an orthogonal diagnostic X-ray set-up for patients with gynecological malignancy: a new application of real-time tumor-tracking system. Radiother Oncol 2004;73:219-22.

13. Kagei K, Shirato H, Nishioka T, Kitahara T, Suzuki K, Tomita M, et al. High-dose-rate intracavitary irradiation using linear source arrangement for stage II and III squamous cell carcinoma of the uterine cervix. Radiother Oncol 1998;47:207-13.
14. Benedet JL, Bender H, Jones H 3rd, Ngan HY, Pecorelli S. FIGO staging classifications and clinical practice guidelines in the management of gynecologic cancers. FIGO Committee on Gynecologic Oncology. Int J Gynaecol Obstet 2000;70:209-62.
15. Cox JD, Stetz J, Pajak TF. Toxicity criteria of the Radiation Therapy Oncology Group (RTOG) and the European Organization for Research and Treatment of Cancer (EORTC). Int J Radiat Oncol Biol Phys 1995;31:1341-6.
16. Kaplan EL, Meier P. Nonparametric estimation from incomplete observations. J Am Stat Assoc 1958;63:457-81.
17. Aydogan B, Mundt AJ, Smith BD, Mell LK, Wang S, Sutton H, et al. A dosimetric analysis of intensity-modulated radiation therapy (IMRT) as an alternative to adjuvant high-dose-rate (HDR) brachytherapy in early endometrial cancer patients. Int J Radiat Oncol Biol Phys 2006;65:266-73.
18. Wahab SH, Malyapa RS, Mutic S, Grigsby PW, Deasy JO, Miller TR, et al. A treatment planning study comparing HDR and AGIMRT for cervical cancer. Med Phys 2004;31:734-43.
19. Schefter TE, Kavanagh BD, Wu Q, Tong S, Newman F, McCourt S, et al. Technical considerations in the application of intensity-modulated radiotherapy as a concomitant integrated boost for locally-advanced cervix cancer. Med Dosim 2002;27:177-84.
20. Low DA, Grigsby PW, Dempsey JF, Mutic S, Williamson JF, Markman J, et al. Applicator-guided intensity-modulated radiation therapy. Int J Radiat Oncol Biol Phys 2002;52:1400-6.
21. Chan P, Yeo I, Perkins G, Fyles A, Milosevic M. Dosimetric comparison of intensity-modulated, conformal, and four-field pelvic radiotherapy boost plans for gynecologic cancer: a retrospective planning study. Radiat Oncol 2006;1:13.
22. Nag S, Erickson B, Thomadsen B, Orton C, Demanes JD, Petereit D. The American Brachytherapy Society recommendations for high-dose-rate brachytherapy for carcinoma of the cervix. Int J Radiat Oncol Biol Phys 2000;48:201-11.
23. Pötter R, Haie-Meder C, Van Limbergen E, Barillot I, De Brabandere M, Dimopoulos J, et al. Recommendations from gynaecological (GYN) GEC ESTRO working group (II): concepts and terms in 3D image-based treatment planning in cervix cancer brachytherapy-3D dose volume parameters and aspects of 3D image-based anatomy, radiation physics, radiobiology. Radiother Oncol 2006;78:67-77.
24. Haie-Meder C, Pötter R, Van Limbergen E, Briot E, De Brabandere M, Dimopoulos J, et al. Recommendations from Gynaecological (GYN) GEC-ESTRO Working Group (I): concepts and terms in 3D image based 3D treatment planning in cervix cancer brachytherapy with emphasis on MRI assessment of GTV and CTV. Radiother Oncol 2005;74:235-45.
25. Chao KS, Williamson JF, Grigsby PW, Perez CA. Uterosacral space involvement in locally advanced carcinoma of the uterine cervix. Int J Radiat Oncol Biol Phys 1998;40:397-403.
26. Tomé WA, Fowler JF. On cold spots in tumor subvolumes. Med Phys 2002;29:1590-8.
27. Tomé WA, Fowler JF. Selective boosting of tumor subvolumes. Int J Radiat Oncol Biol Phys 2000;48:593-9.
28. Lee SW, Back GM, Yi BY, Choi EK, Ahn SD, Shin SS, et al. Preliminary results of a phase I/II study of simultaneous modulated accelerated radiotherapy for nondisseminated nasopharyngeal carcinoma. Int J Radiat Oncol Biol Phys 2006;65:152-60.
29. Shirato H, Oita M, Fujita K, Watanabe Y, Miyasaka K. Feasibility of synchronization of real-time tumor-tracking radiotherapy and intensity-modulated radiotherapy from viewpoint of excessive dose from fluoroscopy. Int J Radiat Oncol Biol Phys 2004; 60:335-41.

ELSEVIER

Int. J. Radiation Oncology Biol. Phys., Vol. ■, No. ■, pp. 1–8, 2010

0360-3016/10/$–see front matter

doi:10.1016/j.ijrobp.2009.10.015

PHYSICS CONTRIBUTION

RADIATION PNEUMONITIS AFTER HYPOFRACTIONATED RADIOTHERAPY: EVALUATION OF THE LQ(L) MODEL AND DIFFERENT DOSE PARAMETERS

GERBEN R. BORST, M.D., PHD.,* MASAYORI ISHIKAWA, PH.D.,† JASPER NIJKAMP, M.SC.,* MICHAEL HAUPTMANN, PH.D.,‡ HIROKI SHIRATO, M.D., PH.D.,† GERARD BENGUA, PH.D.,† RIKIYA ONIMARU, M.D.,† A. DE JOSIEN BOIS, R.T.T.,* JOOS V. LEBESQUE, M.D., PH.D.,* AND JAN-JAKOB SONKE, PH.D.*

*Department of Radiation Oncology, The Netherlands Cancer Institute—Antoni van Leeuwenhoek Hospital, Amsterdam, The Netherlands; †Department of Radiology, Hokkaido University School of Medicine, Sapporo, Japan; and ‡Departments of Bioinformatics and Statistics, The Netherlands Cancer Institute—Antoni van Leeuwenhoek Hospital, Amsterdam, The Netherlands

Purpose: To evaluate the linear quadratic (LQ) model for hypofractionated radiotherapy within the context of predicting radiation pneumonitis (RP) and to investigate the effect if a linear (L) model in the high region (LQL model) is used.

Methods and Materials: The radiation doses used for 128 patients treated with hypofractionated radiotherapy were converted to the equivalent doses given in fractions of 2 Gy for a range of α/β ratios (1 Gy to infinity) according to the LQ(L) model. For the LQL model, different cut-off values between the LQ model and the linear component were used. The Lyman model parameters were fitted to the events of RP grade 2 or higher to derive the normal tissue complication probability (NTCP). The lung dose was calculated as the mean lung dose and the percentage of lung volume (V) receiving doses higher than a threshold dose of xGy (V_x).

Results: The best NTCP fit was found if the mean lung dose, or V_x, was calculated with an α/β ratio of 3 Gy. The NTCP fit of other α/β ratios and the LQL model were worse but within the 95% confidence interval of the NTCP fit of the LQ model with an α/β ratio of 3 Gy. The V_{50} NTCP fit was better than the NTCP fit of lower threshold doses.

Conclusions: For high fraction doses, the LQ model with an α/β ratio of 3 Gy was the best method for converting the physical lung dose to predict RP. © 2010 Elsevier Inc.

LQ model, LQL model, Radiation pneumonitis, Hypofractionation.

INTRODUCTION

An increasing number of radiotherapy departments implement hypofractionated radiotherapy (RT) regimens for pulmonary malignant lesions, encouraged by reports of good tumor control and little toxicity. Consequently, clinical questions concerning normal tissue tolerance dose and the possibility of including multiple targets or irradiating larger lung volumes (*e.g.*, applying multiple treatments or irradiation of larger tumors) are important.

For conventional fractionated radiotherapy, the physical dose can be converted into a biological equivalent dose by using the linear quadratic (LQ) model (1, 2). Historically, the strength of the LQ model for conventional fraction doses is twofold. First, it is a simple mathematical model fitting log cell survival data as a function of the dose. Second, this model enables isoeffect calculations of fractionation schemes with different doses per fraction. However, in 1954, Puck *et al.* had already observed that for the high-dose regions the log cell survival was linear (3). As a result, some modifications have been derived from NSCLC cell lines (4) and other tumor cell lines and animal isoeffect data (5). In general, a nonlinear part (LQ) in the low-dose region and a linear (L) part for the high-dose region differentiated by a transition dose (d_T) was proposed (*i.e.*, LQL model) (6). Since clinical data are lacking, the clinical isoeffect calculations by the LQ model at higher fraction doses remains uncertain, as was comprehensively discussed previously (7–11). Using the LQ model with an α/β ratio of 3 Gy, it was observed that the normal tissue complication probability (NTCP) model predicting radiation pneumonitis (RP) after hypofractionated RT was not different than the NTCP model after conventional

Reprint requests to: Jan-Jakob Sonke, Ph.D., Department of Radiation Oncology, The Netherlands Cancer Institute—Antoni van Leeuwenhoek Hospital, Plesmanlaan 121, 1066 CX Amsterdam, The Netherlands. Tel: +31-20-5122125; Fax: + 31-20-6691101; E-mail: j.sonke@nki.nl

This work has been supported by a UICC International Cancer Technology Transfer Fellowship and a Grant-in-aid from the Japanese Ministry of Education, Culture, Sports, Science, and Technology.

Supplementary material for this article can be found at www.redjournal.org.

Conflicts of interest: none.

Received May 18, 2009, and in revised form Sept 29, 2009. Accepted for publication Oct 7, 2009.

fractionated RT (12). For conventional fractionated RT, the relationship between lung dose and RP has been extensively evaluated (*e.g.*, ref. 13). RP is a serious complication after irradiation, and fatal RP toxicities are also observed after hypofractionated schemes (14).

To evaluate the applicability of the LQ(L) model and normal tissue complication models for higher-dose per fraction, we evaluated the prediction of RP occurring after hypofractionated RT. Different α/β ratios and different d_T values of the LQ(L) models were analyzed, modeling the probability of RP after hypofractionated RT as function of the dose.

METHODS AND MATERIALS

Patients

Patients and treatment schedules were comprehensively described elsewhere (12). In summary, 128 patients were irradiated with hypofractionated RT at the Department of Radiation Medicine of the Hokkaido University School of Medicine, Sapporo, Japan, with 35 Gy in 4 fractions, 40 Gy in 4 fractions, 48 Gy in 8 fractions, 60 Gy in 8 fractions, and 48 Gy in 4 fractions. Twenty patients had multiple targets in one treatment plan (18 patients had two targets, 2 patients had three targets). For 13 patients, multiple treatment plans were made for different targets because of metastasis or recurrence (5 patients had two plans, 4 patients had three plans, and 4 patients had four plans) (for time schedule, dose schedule, and tolerated maximum dose for organs at risk see ref. 12).

Toxicity

RP was prospectively scored according to National Cancer Institute Common Toxicity Criteria (NCI-CTC) version 2, in which grade 2 RP is scored after prescribing steroids for treatment-related toxicity, like progressive shortness of breath combined with typical RP changes on the X-thorax. Grade 3 RP is scored after requiring oxygen. None of the patients whose RP was grade 2 had used steroids before radiotherapy. For all patients, the diagnosis and grade of RP were determined by a radiation oncologist and a pulmonologist experienced in the diagnosis of RP. Patients for whom the diagnosis of RP was unlikely were not included (those with progressive cardiac problems, medical history of receiving oxygen before treatment, and tumor progression).

Dose

Three dimensional treatment plans were made using Focus (CMS, St. Louis, MO), XiO (CMS), or Pinnacle. A convolution superposition algorithm for tissue density heterogeneity was used (plans initially carried out with the Clarkson method were recalculated). Normal lung tissue was defined by computed tomography scan by binary thresholding (thus, excluding the gross tumor volume). Both lungs were considered together as one organ. Four to six noncoplanar beams were used. The beam energy was 4, 6, or 10 MV. Plans were further analyzed with in-house-developed software. The physical dose distribution was converted into the normalized total dose (NTD) distribution (15), using the LQ model. The NTD is defined as the equivalent total dose given in fractions of 2 Gy, as follows:

$$\mathrm{NTD} = D\frac{d + \alpha/\beta}{2 + \alpha/\beta} \tag{1}$$

in which the total dose (D) is the number of fractions multiplied by the dose per fraction (d).

Dose distributions were converted according to Eq. 1 (1) for α/β ratios of 1 Gy, 2 Gy, 3 Gy, 4 Gy, 5 Gy, 7.5 Gy, 10 Gy, and infinity (*i.e.*, physical dose) to evaluate the effect of different α/β ratios. After this conversion for the dose per fraction, we determined different dose-volume parameters from the dose-volume histograms: the mean lung dose (MLD) and the lung volume percentage receiving doses higher than 5 Gy (V_5), 13 Gy (V_{13}), 20 Gy (V_{20}), 40 Gy (V_{40}), and 50 Gy (V_{50}) or, in general, higher than xGy (V_x). For the 33 patients who underwent irradiation for multiple lesions, individual plans were summed after NTD corrections, and image registration had been performed. Time-related recovery of lung tissue was not taken into account for multiple treatments.

The dose response relationship between RP and MLD was modeled by a sigmoid-shaped dose effect relationship according to Lyman (16). The NTCP can be calculated from the MLD (17) according to the equation:

$$\mathrm{NTCP} = \frac{1}{\sqrt{2\pi}}\int_{-\infty}^{t} e^{\frac{-x^2}{2}}dx \tag{2}$$

with $t = \frac{MLD - TD_{50}}{m \cdot TD_{50}}$ in which TD_{50} represents the dose for a 50% NTCP and m is the (inverse) steepness parameter in the standard formulation of the Lyman model. Similarly for the V_x parameter, Eq. 2 was used with $t = \frac{V_x - V_{x50}}{m \cdot V_{x50}}$ such that the V_{x50} represents the V_x parameter for a 50% NTCP.

Modification of the LQ model to the LQL model

We adapted the LQ model (LQL) by applying a two-component model proposed by Park *et al.* (4) (Fig. 1). For the low-dose range, the total dose is corrected according to the LQ model by using Eq. 1 according to the best α/β ratio. For the high-dose range, the log survival curve is assumed to be linear. The slope of the linear part is determined by the derivative of the LQ curve at the cut-off value between the linear-quadratic part and the linear part (*i.e.*, the transition dose [d_T]) (Fig. 1, also see Appendix E1) resulting in the equation:

$$\mathrm{NTD} = D\frac{\alpha/\beta + 2d_T - \frac{d_T^2}{d}}{2 + \alpha/\beta} \tag{3}$$

In contrast to nomenclature in the literature, we propose to use the denotation of a lower-case letter (d_T) because this transition dose refers to the dose-per-fraction correction. We converted the dose distributions for d_T values of 0 Gy, 5 Gy, 7 Gy, and 9 Gy and subsequently calculated the MLD (not the V_x) from these dose distributions (*i.e.*, MLDLQL).

Statistics

The terms TD_{50} and m were estimated by maximizing the logarithm of the likelihood function (17), as follows:

$$\begin{aligned}\ln(L) &= \ln\left(\prod_{i=1}^{N} Li\right) = \sum_{i=1}^{N} \ln(L_i) \\ &= \sum_{i=1}^{N} [ep_i \ln(P_i) + (1\text{-}ep_i)\ln(1\text{-}P_i)]\end{aligned} \tag{4}$$

where P_i ($i = 1,\ldots, N$) represents the predicted NTCP and ep_i is the observed binary outcome (0 = an RP grade of ≤ 1, and 1 = an RP grade of ≥ 2) for patient i.

The confidence intervals (CI) of the fitted parameters were calculated using the profile likelihood method (18). These CI were

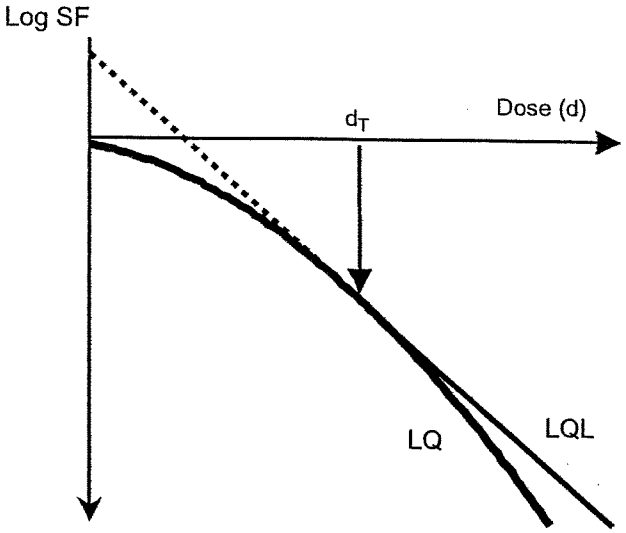

Fig. 1. Schematic representation of the log survival curve as a function of the dose according to the LQL model is shown. Below the transition dose (d_T), the curve is linear quadratic (the LQ model). Above d_T , the log survival curve is linear, whereby the slope is determined by the asymptote of the LQ model at dose d_T.

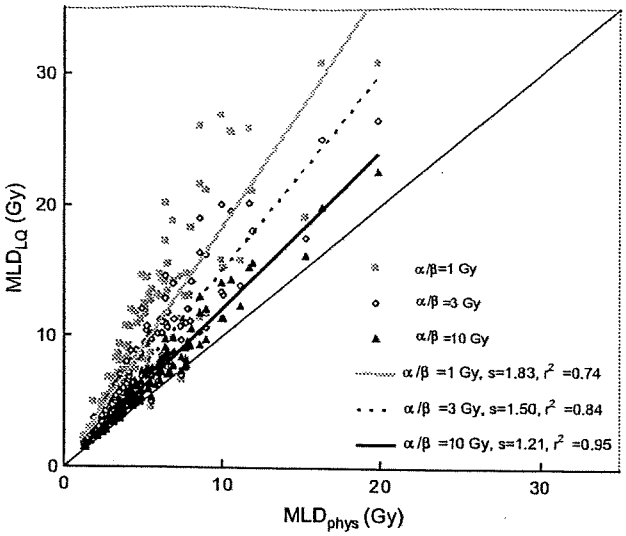

Fig. 2. The MLDLQ calculated according to the LQ model with α/β ratios of 1 Gy, 3 Gy, 10 Gy plotted as function of the MLD_{phys}. The straight line with a slope of 1 represents the equivalent line where MLDLQ equals MLD_{phys}. The other lines represent the best fit through the data with a zero intercept; s represents the slope and *r* the regression coefficient.

calculated by finding the points in the parameter space where the ln(L) values are Δln(L) lower than $\ln(L_{max})$ (*e.g.*, for the 95% CI the value of Δln[L] is 1.92, corresponding to half of the 95% percentile of the cumulative chi-square value for 1 degree of freedom).

In order to evaluate which α/β ratio would give the maximum likelihood estimation, a profile likelihood approach of the best NTCP fit was performed according to α/β ratios in the range of 1 Gy to infinity. This analysis was performed only for the MLD (*i.e.*, the corrected mean lung dose [MLDLQ]).

Converting the dose according to the LQL model, we used an α/β ratio of 3 Gy. The LQ and the LQL models are nested, since the three-parameter (TD_{50}, *m* , and d_T) MLDLQL model reduces to the two-parameter (TD_{50}, *m*) MLDLQ model when d_T goes to infinity (or at least becomes higher than the highest dose-per-fraction value in the data set) (Fig. 1). According to the LQL model, the doses were converted with d_T values of 0, 5, 7, and 9 Gy. The NTCP model fit using the MLDLQL was compared to the NTCP model fit with the MLDLQ, using the maximum likelihood ratio test, since the two models were nested (19). For this analysis, this requires that twice the difference of the log likelihoods between the two models should be larger than the quantile of a chi-square distribution with 1 degree of freedom (*i.e.*, 3.84/2) to be significantly different.

For regression analysis, the slope of the linear regression(s) with a zero intercept was used to assess the relationship between different parameters. A two-tailed *p* value of <0.05 was considered to be statistically significant.

RESULTS

The crude incidence of RP was 10.9% (14 events in the group of 128 patients). One patient was diagnosed with a grade 3 RP, all other patients were diagnosed with grade 2 RP.

MLD corrected for different α/β ratios

The relationships between the MLD calculated with an α/β ratio of infinity (MLD_{phys}) and of 1 Gy (MLD_1), 3 Gy (MLD_3), and 10 Gy (MLD_{10}) are illustrated in Fig. 2. The MLDLQ calculated with a low α/β ratio is higher than the MLDLQ calculated with a higher α/β ratio, as expected. A linear fit of the data (with zero intercept) resulted in the following relationships and correlations; $MLD_1 = 1.83 \times MLD_{phys}$ ($r^2 = 0.74$), $MLD_3 = 1.50 \times MLD_{phys}$ ($r^2 = 0.84$), and $MLD_{10} = 1.21 \times MLD_{phys}$ ($r^2 = 0.95$), respectively. Two patients were located under the equality line. These two patients were also irradiated at a target in the mediastinum with a more fractionated scheme whereby the high-dose region in the lung tissue received less than 2 Gy.

To evaluate the effect of the dose per fraction, the MLD_1 and the MLD_3 values were plotted as a function of the MLD_{phys} (Fig. 3) for each dose per fraction separately for patients irradiated on one single target. Because only 3 patients received 35 Gy/4 fractions, these patients were excluded. As expected, the slopes of the linear regression of the higher dose per fraction schedules (10 Gy and 12 Gy per fraction) were higher than for the lower dose per fraction schedules (6 Gy and 7.5 Gy per fraction). In addition, the slopes for the α/β ratio of 1 Gy was higher than the slope for the α/β ratio of 3 Gy for each dose per fraction. All correlations were significant with a *p* of <0.001.

The MLD calculated according to the LQL model (MLDLQL) with a d_T of 5 Gy is shown as a function of the MLD_3 in Fig. 4. For patients with a high MLD_3 and who were irradiated with a high dose per fraction, larger differences between the MLD_3 and the MLDLQL were observed than for other patients (Fig. 4).

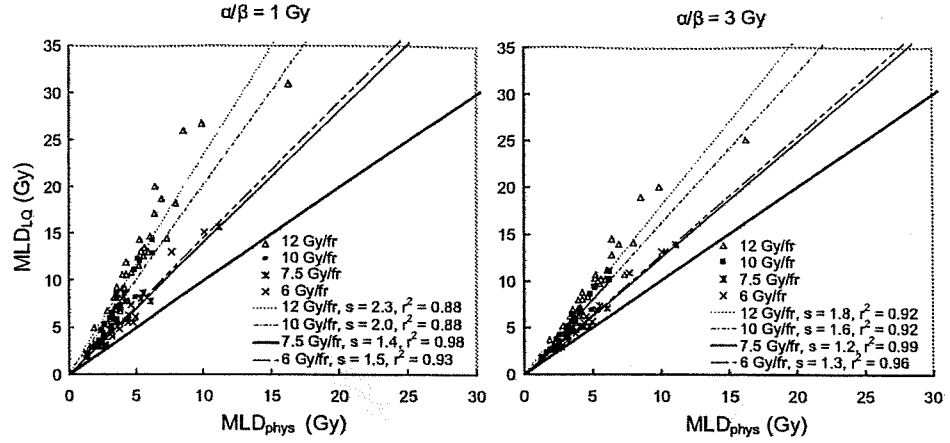

Fig. 3. The MLD_1 and MLD_3 as a function of the MLD_{phys} are plotted for different fractionation schemes. The straight line with a slope of 1 represents the equivalent line where MLDLQ equals MLD_{phys}. The other lines represent the best fit through the data with a zero intercept; s represents the slope and *r* the regression coefficient.

NTCP for different α/β ratios and the LQL and V_x models

Optimizing the LQ NTCP model as a function of the *m*, TD_{50} , and α/β ratio revealed that the highest maximum log likelihood was found at an α/β ratio of 3 Gy (with TD_{50} = 20.8 Gy and *m* = 0.45). All other evaluated α/β ratios had lower maximum log likelihoods (Fig. 5) but were within the 95% CI of the NTCP fit with an α/β ratio of 3 Gy. The largest difference was found between the NTCP fit with an α/β ratio of 3 Gy and the NTCP fit with an α/β ratio of infinity (*i.e.*, physical dose) (with TD_{50} = 14.6 Gy, and *m* = 0.48), but this was not significant ($p = 0.07$) (Fig. 6).

Evaluating the NTCP model according to the LQL model with a d_T value of 5 Gy, the maximum log likelihood was lower than the MLD_3 NTCP LQ model fit. The LQL NTCP fit parameters TD_{50} of 19.5 Gy and *m* = 0.46 were not significantly different from the LQ fit parameters ($p = 0.28$). The NTCP model according to the LQL model with a d_T of 7 Gy and a d_T value of 9 Gy was approaching the MLD3 NTCP LQ model fit, as expected, because only a limited part of the distribution of doses per fraction was larger than these d_T values. The NTCP according to the LQL model with a d_T value of 0 Gy was, as expected, similar to the MLD_{phys} NTCP LQ model fit.

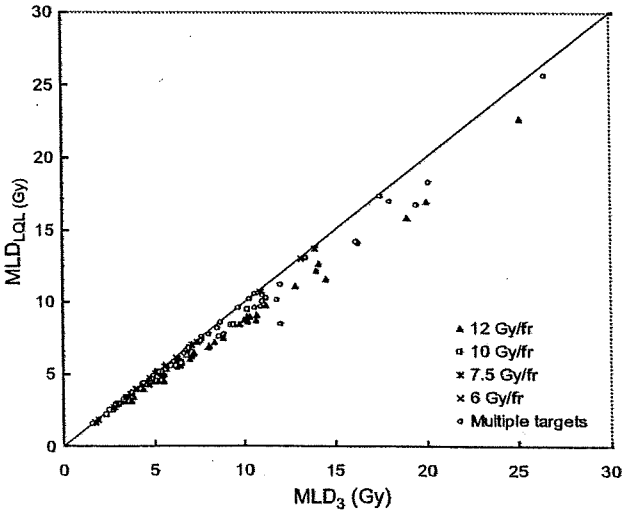

Fig. 4. The MLDLQL as a function of MLD_3 is shown plotted for different fractionation schemes. The straight line with a slope 1 represents the equivalent line where MLDLQL equals MLD_3.

For the V_x (calculated with the LQ model with an α/β ratio of 3 Gy), the maximum likelihood profile approach revealed that the highest likelihood (*i.e.*, best fit) is achieved with a threshold dose of 50 Gy. The V_{50} calculated with the LQL model had lower log likelihood parameters (worse fits), although these differences were not significant ($p = 0.16$ for d_T = 5 Gy and $p = 0.21$ for d_T = 7 Gy). For all other V_x values, similar results were observed (data not shown).

The values V_5, V_{13} , and V_{20} were outside the 95% CI of V_{50} (Table 1). Because one patient had 0% of the lung volume receiving doses higher than 60 Gy (corrected for an α/β ratio of 3 Gy), we did not evaluate V_x values higher than 50 Gy.

DISCUSSION

Our results showed that the NTD-corrected MLDLQ calculated with an α/β ratio of 3 Gy was the best parameter to fit the NTCP model to the observed incidence of RP after hypofractionated RT. These data suggest that a correction for the dose per fraction after hypofractionated radiotherapy should be performed similar to conventional fractionated schemes (*i.e.*, LQ model and an α/β ratio of 3 Gy [*e.g.*, see ref. 20]). Other tested α/β ratios or a modification of the LQ model (by introducing a linear relation after a threshold dose d_T of 5 Gy or higher) deteriorated the predictive value of the lung dose but were within the 95% CI of the NTCP LQ model fit with an α /β ratio of 3 Gy. The nonsignificant differences in the NTCP fits might be explained by the strong correlations between the corrected dose parameters.

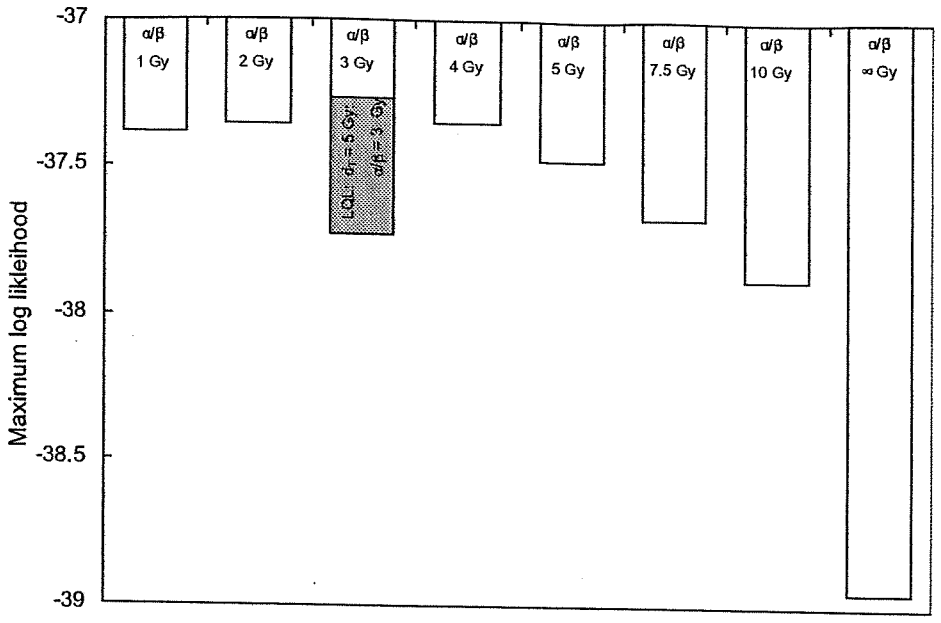

Fig. 5. The maximum log likelihood of the NTCP fit for the MLD calculated for different α/β ratios is shown. In the grey rectangle the maximum log likelihood of the NTCP fit based on the MLD calculated with the LQL model (with an α/β ratio of 3 Gy and a d_T of 5 Gy) is indicated next to the MLD_3. The maximum log likelihood of the NTCP fit based on the MLD calculated with the LQL model (with an α/β ratio of 3 Gy and a d_T of 5 Gy) is indicated next to the MLD_3.

Since the dose per fraction in hypofractionated RT is considerably larger than 2 Gy, a substantial volume of lung tissue received more than 2 Gy per fraction. Because the MLDLQ is expressed as 2-Gy equivalents, the MLDLQ is, therefore, expected to be larger than the MLD_{phys}. Evaluating different α/β ratios resulted in different relationships between the MLDLQ and the MLD_{phys}. By the nature of the LQ model, for lower α/β ratios and higher fraction doses, the difference between the MLDLQ and MLD_{phys} increased, and for higher α/β ratios, the MLDLQ approached that of the MLD_{phys}. Because of the strong correlation between the MLDLQ and the MLD_{phys}, it might be questioned whether the physical dose can be used to estimate complication probabilities. However, our results confirm also that after hypofractionation, the physical dose should not be used for calculation of toxicity probabilities.

By calculating the MLD, the local dose in the lungs is weighted according to a linear local dose-effect relation. In contrast, for the V_x the local dose-effect relationship is considered a binary effect whereby no damage is taken into account below the threshold dose of xGy and a full damage above the threshold dose of xGy. Different dose volume parameters and their mutual relationships have not previously been evaluated for hypofractionated RT. Since the dose effect relationship expressed by the MLD and Vx are based on different parameters (*i.e.*, models are not nested), a direct comparison of the NTCP fits via a log likelihood ratio approach is not possible. Including these parameters (MLD, V_5, V_{13}, V_{20}, and V_{40}) in a multivariate logistic regression analysis revealed that only the MLD was significantly associated with RP (data not shown). However, these data should be interpreted with caution since it is known from studies with conventional fractionated RT evaluating clinical and dose factors predicting RP that there is a large heterogeneity of results (21–32), whereby no validation was performed. One collaborative study from Duke University and The Netherlands Cancer Institute developed a prospective method to predict RP from dose and clinical parameters in one group of patients, but validation failed in another group of patients (33).

The validity of the LQ model for both clonogenic cell survival as clinical isodose calculations for higher dose per fraction was discussed previously; Hall and Brenner (11) estimated from the isoeffect data of van der Kogel (34) (late-responding damage to the rat spinal cord) and Douglas and Fowler (35) (acute damage to the mouse skin) that the LQ model would be valid for single doses up to 20 Gy. According to this estimation, Fowler *et al.* (9) extrapolated the relationship between RP and MLD, as determined for conventionally treated patients, to hypofractionated schemes. Unfortunately, clinical data were lacking to validate such an extrapolation. Concerning RP (or other clinical toxicity endpoints), it might be questioned whether the applicability of the LQ model for these fraction doses can be answered by clinical studies. For example, the high number of (noncoplanar) beams results in an irradiation dose to healthy (lung) tissue that will be much smaller than the maximum dose. In addition, the relative volume of healthy tissue receiving such a high dose is limited by current advanced radiotherapy techniques (*e.g.*, intensity-modulated RT and Image guided RT [IGRT]). Moreover, the purpose of these techniques is to avoid high doses to normal tissues.

Guerrero *et al* (5) developed a modification of the LQ model by extending the LQ model with a protraction factor, based on the lethal-potentially lethal (LPL) model, which is

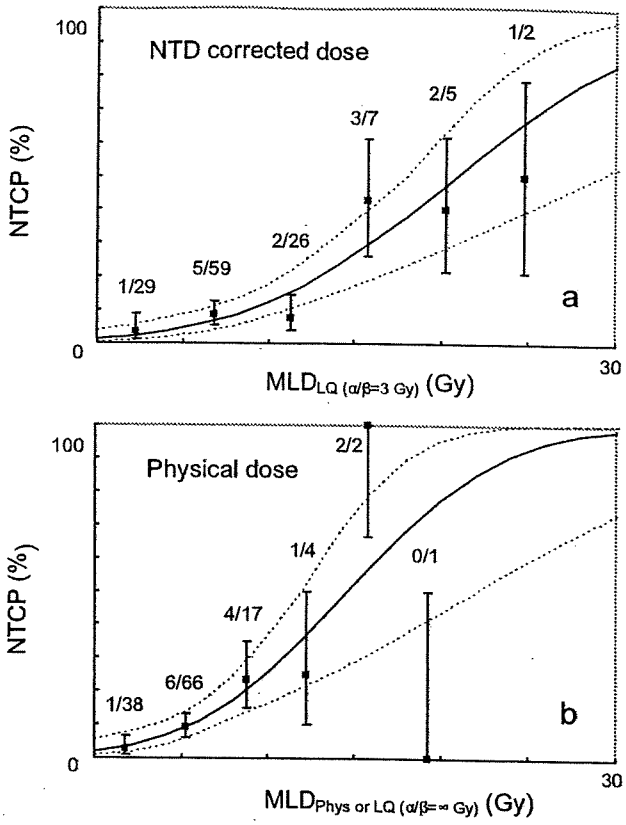

Fig. 6. (Top) The NTCP fit (solid line) is shown as a function of the MLD calculated according to the LQ model and an α/β ratio of 3 Gy with the 68% CI (dotted lines) (TD_{50} = 20.8 Gy, m = 0.45). The number of events and number of patients are indicated. (Bottom) The NTCP fit (solid line) is shown as a function of the physical MLD (*i.e.*, LQ model and an α/β ratio of infinity) with the 68% CI (dotted lines) (TD_{50} = 14.6 Gy, m = 0.48). The number of events and number of patients are indicated.

supposed to be superior, describing log cell survival data in the higher dose region (36). This modification was based on cell survival and animal toxicity data. The authors observed a wide range of dose values where the LQ started to deviate from the LPL model (cell lines 0.6 Gy to 37.7 Gy; animal toxicity data 2.6 Gy to 100 Gy). It was shown that this modification results in a LQ model with a linear extension of the log cell survival as function of the dose for the high-dose range by Carlone *et al.* (6), and they proposed to name this model the linear-quadratic-linear (LQL) model. Elaborating this discussion in the clinical setting, we evaluated the LQL model with clinical data by using the simpler but similar method proposed by Park *et al.* (4), using a linear extension of the log cell survival as a function of the dose for doses higher than the threshold (*i.e.*, transition dose d_T). For a d_T of 5 Gy, we observed a (nonsignificant) worse NTCP fit. For higher d_T values, the LQL NTCP fit approached the LQ NTCP fit; the differences between the MLDLQL and MLDLQ are becoming smaller because less lung tissue dose will be recalculated according to the linear part of the LQL model (dose larger than the d_T). Last, if the d_T is larger than the largest fraction doses, the MLDLQL equals the

Table 1. The optimized V_{x50} and m for the different V_x values with the 95% CI

V_x value	V_{x50} (95% CI)	m (95% CI)	Maximum log likelihood
V_5	65.4 (49.0–121.0)†	0.46 (0.34–0.66)	−39.40
V_{13}	39.2 (30.0–77.0)	0.48 (0.36–0.67)	−39.77
V_{20}	30.6 (23.0–57.0)	0.50 (0.37–0.68)	−39.63
V_{40}	15.9 (13.0–27.0)	0.48 (0.37–0.65)	−38.12
V_{50}	13.1 (11.0–21.0)	0.48 (0.37–0.65)	−37.04

The V_{x50} and m representing the value of V_x (%) with a 50% Normal Tissue Complication Probability (NTCP) and steepness parameter, respectively.

† Note that the upper boundary of 95% CI exceeds the 100% lung volume due to the approximation in the statistical method applied, whereas in mathematical and clinical terms, the upper limit is 100%.

MLDLQ. Another mathematical model to describe the cellular response as function of the irradiation dose is the linear quadratic cubic (LQC) (37) model, whereby the cubic term is negative. This LQC model also has a (more) linear response in the high-dose region, approximating that of the LPL model. As with the LQL model, the LQC model is mathematically simpler than the LPL model, with only one additional parameter (as in the LQL model).

At the NKI (and many other institutes), the hypofractionated schedule that is mainly given is 3 × 18 Gy. Unfortunately, the patients treated at the NKI could not be included in the current analysis. The first reason for this is the limited follow-up of a substantial part of these patients. Second, the patients with sufficient follow up (>1 year) had lung doses only in the lower MLD range, resulting in low incidences of RP. Consequently, these patients cannot be of additional value for this type of analysis. However, the relationship between the MLDLQL as a function of the MLDLQ for

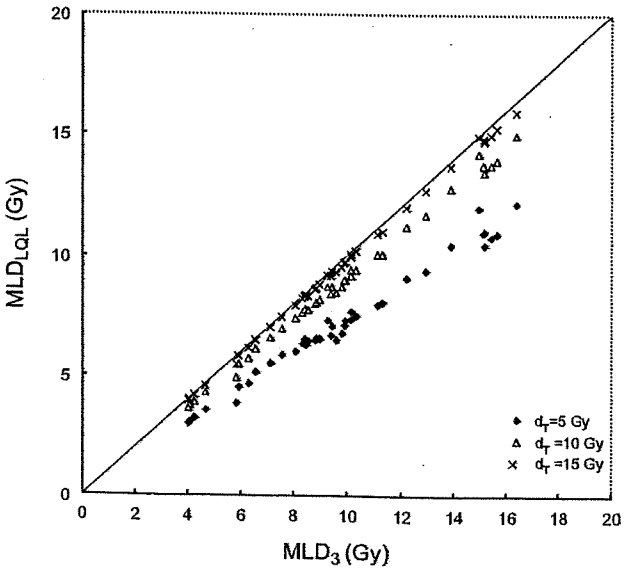

Fig. 7. For patients treated at the NKI-AVL, the MLDLQL is plotted as a function of MLD_3 for a d_T of 5 Gy, a d_T of 10 Gy, and a d_T of 15 Gy. The straight line with a slope 1 represents the equivalent line where MLDLQL equals MLD_3.

higher transition doses than those used in current analysis could be evaluated. As illustrated in Fig. 7, only a d_T of about 10 Gy or lower results in a difference between the MLDLQL and the MLDLQ. Introduction of a higher d_T would lead to imperceptible differences between the MLDLQ and the MLDLQL. Consequently, it might be questioned whether a higher d_T can be clinically evaluated with respect to RP in the future due to limited amount of lung tissue receiving high doses. Irradiation of healthy lung tissue of animals with increasing fraction sizes, which could be possible in the future with advances in preclinical irradiation techniques, might facilitate resolving this issue.

We evaluated the LQL model by using an α/β ratio of 3 Gy, which did not improve the NTCP fit to the data. Although the slope of the linear component is dependent of both the d_T and the α/β ratio, we did not analyze the LQL model with other α/β values. The first reason for this is that evaluations of the LQL model with α/β ratios close to 3 Gy would not affect the NTCP fit significantly according to current data. Second, for (much) higher α/β values, the LQL model approaches the LQ model (for α/β equal to infinity the LQL and LQ model both are becoming the L [linear] model). Third, for lung tissue, an α/β value of 3 to 4 Gy is an accepted value, converting doses in the lower dose range (38-42).

Predictive models based on clinical data are as good as the clinical data. Consequently, the limitations of this study should be stressed. We discussed the clinical limitations of our study comprehensively previously (12). First, the study was a retrospective univariate analysis evaluating RP grade $\geq$2. Second, although the assessment of RP was carefully performed, the prescription of steroids and oxygen relies on the intention to treat of the physician. Third, only one grade 3 RP was scored, and the duration of the RP grade 2 treatment was not registered. Therefore, no dose response analysis could be performed regarding the severity of the radiation-induced toxicity. Another discussion point is whether the time interval between the subsequent treatments should be taken into account. As discussed previously (12), we did not considered any repair between the treatments. A mouse study suggested that for higher doses per fraction, less recovery might be expected (43). Moreover, limited clinical data showed that patients are experiencing a high probability of RP after reirradiation (44).

Besides the reliability of NTCP modeling on the robustness of the clinical data, some assumptions have to be made for (NTCP) modeling in general. First, a NTCP model based on one (dose) characteristic disregards all other factors influencing the probability to develop toxicity (*e.g.*, genetic variability and/or comorbidity) for one individual patient. Second, to evaluate clinically applicable dose parameters, dose-volume histograms are reduced to simple parameters (*e.g.*, MLD and V_x), whereby a (biological) background is assumed but questionable. Third, the limited number of patients included in the current study might have caused the fact that a real intrinsic difference between these parameters was not apparent with statistical significance.

CONCLUSIONS

In conclusion, with our study we provide clinical toxicity data for the discussion of the applicability of current radiobiological models for higher doses per fraction. We observed that the LQ model was valid (with an α/β ratio of 3 Gy for lung tissue) to recalculate the physical dose into biologically equivalent dose and that the biological dose should be used for estimating toxicity probabilities. The LQL model did not improve the prediction of RP. This might be due to the limitations of our study and/or to (still) unknown fundamental mechanisms complicating the translation of mathematical models developed with cell survival data into clinical data. With currently used fraction doses of up to 18 Gy, substantially different results are not expected, but this should be confirmed in future evaluations.

REFERENCES

1. Fowler JF. The first James Kirk memorial lecture. What next in fractionated radiotherapy? *Br J Cancer Suppl* 1984;6:285–300.
2. Tucker SL. Tests for the fit of the linear-quadratic model to radiation isoeffect data. *Int J Radiat Oncol Biol Phys* 1984;10:1933–1939.
3. Puck T, Marcus P. Action of x-rays on mammalian cells. *J Exp Med* 1956;103:653–666.
4. Park C, Papiez L, Zhang S, *et al.* Universal survival curve and single fraction equivalent dose: useful tools in understanding potency of ablative radiotherapy. *Int J Radiat Oncol Biol Phys* 2008;70:847–852.
5. Guerrero M, Li XA. Extending the linear-quadratic model for large fraction doses pertinent to stereotactic radiotherapy. *Phys Med Biol* 2004;49:4825–4835.
6. Carlone M, Wilkins D, Raaphorst P. The modified linear-quadratic model of Guerrero and Li can be derived from a mechanistic basis and exhibits linear-quadratic-linear behaviour. *Phys Med Biol* 2005;50:L9–L13.
7. Barendsen GW. Dose fractionation, dose rate and iso-effect relationships for normal tissue responses. *Int J Radiat Oncol Biol Phys* 1982;8:1981–1997.
8. Denekamp J, Waites T, Fowler JF. Predicting realistic RBE values for clinically relevant radiotherapy schedules. *Int J Radiat Biol* 1997;71:681–694.
9. Fowler JF, Tome WA, Fenwick JD, *et al.* A challenge to traditional radiation oncology. *Int J Radiat Oncol Biol Phys* 2004;60:1241–1256.
10. Hall EJ, Brenner DJ. The radiobiology of radiosurgery: Rationale for different treatment regimes for AVMs and malignancies. *Int J Radiat Oncol Biol Phys* 1993;25:381–385.
11. Marks LB. Extrapolating hypofractionated radiation schemes from radiosurgery data: Regarding Hall *et al.*, *Int J Radiat Oncol Biol Phys* 1991;21:819–824 and Hall and Brenner, *Int J Radiat Oncol Biol Phys* 1993;25:381–385. *Int J Radiat Oncol Biol Phys* 1995;32:274–276.
12. Borst GR, Ishikawa M, Nijkamp J, *et al.* Radiation pneumonitis in patients treated for malignant pulmonary lesions with